Uncovering anti-inflammatory activity of ginsenoside Rg1 in wound-inured zebrafish model by GC-MS-based chemical profiling

Hsu, S.; He, M.; Salomé-Abarca, L.F.; Choi, Y.H.; Wang, M.

Article published online: 2025-06-16

Uncovering Anti-Inflammatory Activity of Ginsenoside Rg1 in a Wound-Inured Zebrafish Model by GC-MS-based Chemical Profiling

Authors

Su-Jung Hsu[1,2*], Min He[3,4*], Luis Francisco Salomé-Abarca[5], Young Hae Choi[1], Mei Wang[4,6,7,8]

Affiliations

1 Natural Products Laboratory, Institute of Biology, Leiden University, Leiden, Netherlands
2 School of Pharmacy, Taipei Medical University, Taipei City, Taiwan
3 Northeast Research Asia Institute of Traditional Chinese Medicine, Changchun University of Chinese Medicine, Changchun, P. R. China
4 Leiden University-European Center for Chinese Medicine and Natural Compounds, Leiden University, Leiden, Netherlands
5 Colegio de Postgraduados, Posgrado de Recursos Genéticosy Productividad-Fruticultura. Carretera México-Texcoco Km. 36.5, Montecillo, Texcoco de Mora, México
6 Naturalis Biodiversity Center, Leiden, Netherlands
7 SU Biomedicine, Leiden Bio Science Park, Leiden, Netherlands
8 Northwest University, Xi'an, China

Keywords

Panax ginseng, ginsenosides Rg1, metabolomics, gas chromatography/mass spectrometry, wound-injured inflammation, zebrafish

received	August 27, 2024
accepted after revision	May 11, 2025
published online	June 16, 2025

Bibliography

Planta Med 2025; 91: 609–620
DOI 10.1055/a-2606-6705
ISSN 0032-0943

Georg Thieme Verlag KG, Oswald-Hesse-Straße 50, 70469 Stuttgart, Germany

Correspondence

Dr. Mei Wang
Naturalis Biodiversity Center
Darwinweg 2, 2333 CR Leiden, Netherlands
Phone: + 31 65 32 29 672, Fax: + 31 71 51 75 217
mei.Wang@subiomedicine.com

Supplementary Material is available under https://doi.org/10.1055/a-2606-6705

ABSTRACT

There is growing evidence highlighting the pivotal role of cellular metabolic adaptation in governing diverse immune responses, as well as the capacity of immune cells to alter metabolic preferences. In both scenarios, the prospect of leveraging bioactive compounds to induce metabolic reprogramming emerges as a novel adjuvant strategy for clinical immunotherapy. Rg1, a major active ginsenoside found in ginseng roots, has the potential to function as a glucocorticoid receptor agonist. Unraveling the intricate relationship between anti-inflammatory functions and the metabolic effects of ginsenosides and glucocorticoids may contribute to the identification of metabolic biomarkers associated with anti-inflammation. This research aims to determine endogenous metabolic response differences evoked by Rg1 and glucocorticoids underlying *in vivo* anti-inflammatory responses. The metabolic impact, particularly on primary metabolites, was assessed in zebrafish embryos using gas chromatography–mass spectrometry (GC-MS) in conjunction with metabolic pathways analysis via the KEGG pathway database. Our results indicated that Rg1 possesses a similar effect in alleviating inflammation in treating injured zebrafish as beclomethasone. The anti-inflammatory effects of Rg1 are achieved by inhibiting the neutrophils and macrophages toward the amputated edges and upregulating gene expression associated with pro-inflammatory cytokines. The anti-inflammatory effects of Rg1 also include changes in fatty-acid metabolism and downstream aromatic amino acids in the TCA cycle. Therefore, Rg1 may be a promising drug candidate for treating inflammatory responses and a valuable supplement for enhancing immune regulation.

* These authors contributed equally to the manuscript.

Introduction

Inflammatory processes and immune response are considered as primary targets for drug therapies due to their importance in a broad spectrum of chronic inflammatory disorders, including rheumatoid arthritis, psoriasis, Crohn's disease, and bronchial asthma, among others [1]. The persistent challenge of achieving a satisfactory therapeutic response has spurred ongoing efforts to explore novel and effective treatments. Currently, glucocorticoids (e.g., beclomethasone) are the common anti-inflammatory and immuno-suppressing agents to treat several acute and chronic inflammatory diseases in clinic practices, including asthma, Crohn's disease, rheumatoid arthritis, and even some cancers [2]. The pharmacological mechanism involves the regulation of inflammatory genes expression such as NF-κB and Stat3 [3], via the glucocorticoid receptor (GRs), a member of the nuclear receptor family, in response to glucocorticoid signaling. However, glucocorticoids have a wide-ranging influence, extending beyond their anti-inflammatory actions. They also regulate multiple immune responses, metabolism, growth, reproduction, vascular tone, bone formation, and brain function. The abuse of glucocorticoids, especially in chronic administration, may lead to severe undesirable side effects, including alteration of glucose metabolism, osteoporosis, affecting wound healing and with skin and muscle atrophy, diabetes, abdominal obesity, glaucoma, growth retardation in children, and hypertension [4, 5]. Consequently, there is significant interest in finding new anti-inflammatory drug candidates with reduced side effects, especially from natural resources such as plants used in traditional medicine.

In the context, *Panax ginseng* C. A. Mayer (Araliaceae, also called "ginseng" or "renshen") is a well-established traditional medicine in Asian countries. The roots are the most commonly utilized organ of ginseng, and they contain a plethora of steroidal saponins (ginsenosides), exhibiting structural and functional similarities to glucocorticoids. Notably, Rg1 is the most abundant ginsenoside in ginseng, and it has been recently confirmed as a GR ligand that competes against glucocorticoids for binding to the glucocorticoid receptor, suggesting its potential as a substitute for glucocorticoids [6]. Despite these findings, the latent cellular and molecular mechanisms underlying the effects of ginseng and ginsenosides, particularly in regulating immune responses at metabolic level, remain to be investigated.

Metabolite analysis is a key approach for monitoring drug efficacy, endogenous and drug-related small molecules in various matrixes [7]. Recent technological advances have improved the sensitivity and robustness of such analyses, enabling more data for metabolomics studies, which provided them with popularity in life sciences. By analyzing bio-fluids such as urine, serum, plasma, and cerebrospinal fluid, metabolomics studies assist in identifying disease biomarkers, aid diagnosis, and evaluate drug efficacy for metabolic and inflammatory diseases, including cancer, cardiovascular disease (CVD), and neurological diseases, among others. [8, 9]. Between diverse analytical platforms for metabolomics, GC-MS stands out for profiling primary metabolites, including carbohydrates, fatty acids, and amino acids. Its robustness and simplicity in identifying metabolites through reliable databases is an advantage for primary metabolite profiling [10]. Thus, considering that the intake of anti-inflammatory agents may affect predominantly the levels of endogenous primary metabolites, GC-MS is considered as a judicious choice for investigating the endogenous metabolic changes regarding inflammatory processes.

Stringent European and American animal welfare regulations, prioritizing animal protection, need to explore alternative models to rodents for plant and herbal pharmacological studies. Among all potential alternatives, the zebrafish (*Danio rerio*) model is one of the most promising. This model is a viable substitute due to the extensive homology in genomic sequencing between zebrafish and mammalian species (more than 70%), including human beings [11]. The zebrafish preserves aspects of multiple organ structures, as well as an immune system, enhancing its widespread applications in pharmacological evaluations [12]. Zebrafish embryos necessitate microgram quantities of test compounds due to their smaller mass and size, which also helps to reduce maintenance costs. These have been utilized across various research fields, including toxicological studies [13], investigations into adiposity [14], non-alcoholic steatohepatitis [15], atherosclerosis [16], skin cancer [17], intestinal inflammation [18], and research on obesity and diabetes [19], among others. Remarkably, some studies have highlighted the functional similarity of the zebrafish glucocorticoid receptor to that of humans, surpassing the likeness observed in mouse models [20].

Our previous investigation unveiled the anti-inflammatory effects of ginsenoside Rg1 in injured zebrafish, without eliciting glucocorticoid-like side effects that impede tissue regeneration [21]. However, considering the glucocorticoid-like side effect in metabolic homeostasis imbalance, whether the Rg1 regulates endogenous metabolism differently from the glucocorticoids is worth exploring. Therefore, based on the information mentioned above, we applied GC-MS-based metabolomics to monitor metabolic differences regulated by the Rg1 and compare it with that of beclomethasone against the inflammatory response of 3 dpf zebrafish larvae. Subsequently, networks for typical metabolic pathways comparison were generated. This study could assist in the interpretation of the biological mechanism of ginsenosides with its similarity and/or dissimilarity with glucocorticoids that were revealed in wound-injured zebrafish.

Results

The zebrafish larva with the tail-fin amputation model is commonly employed to investigate acute inflammatory responses involving leukocyte migration. The transgenic fish line Tg (mpx: GFPi114/mpeg1: mcherry-FumsF001) facilitates the visualization of immune cell migration, including neutrophils and macrophages, under fluorescence microscopy. Our results demonstrated that tail-fin amputation in 3-day-old zebrafish larvae induced neutrophil and macrophage migration to the amputated site within 4 hours of the procedure (▶ **Fig. 1 b**). Pre-surgical treatment with Rg1 significantly suppressed the accumulation of both neutrophils and macrophages at the amputated site, while beclomethasone significantly reduced the infiltration of neutrophils but exhibited no effect on the cell number and migration of macrophages (▶ **Fig. 1 c**).

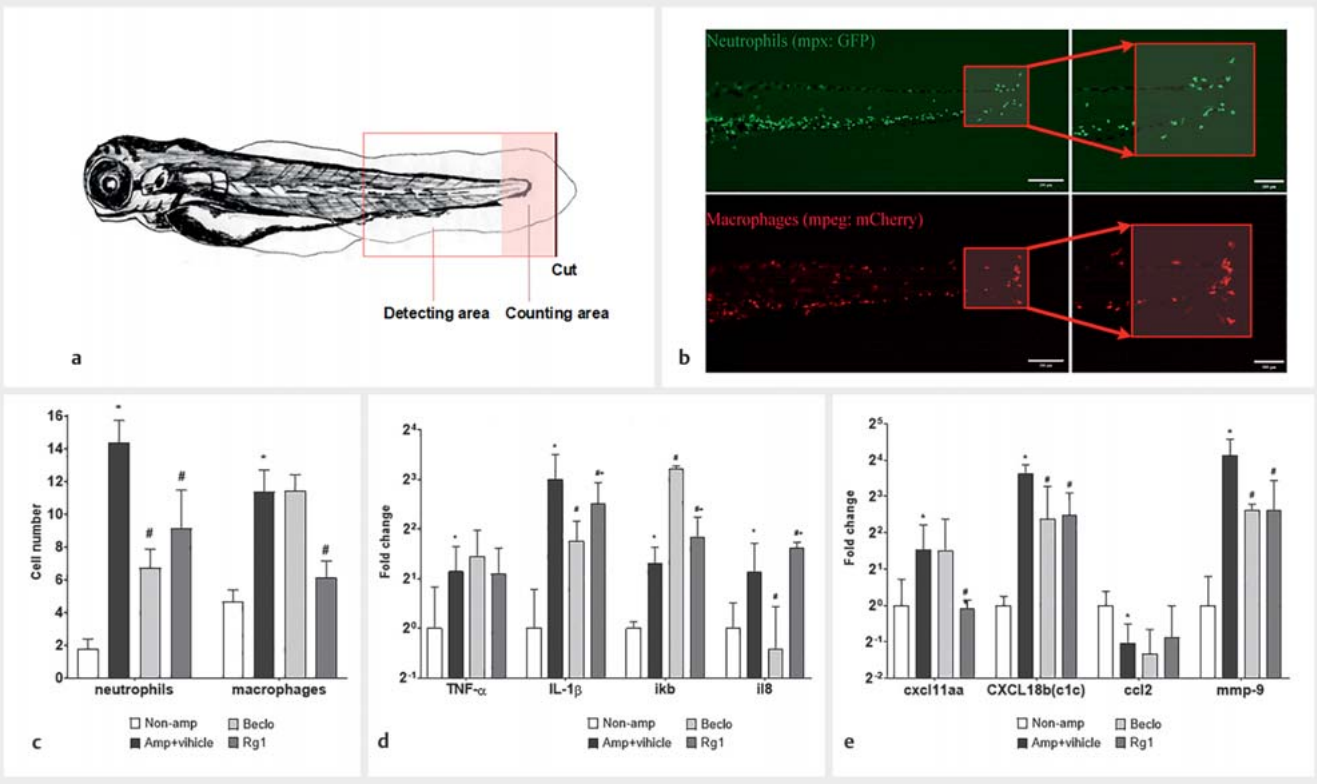

▶ **Fig. 1** Anti-inflammatory effect of Rg1 on the tail-fin amputated zebrafish larvae. **a** Location of tail-fin amputation and analytical area of zebrafish larvae at 3-day post fertilization. **b** Fluorescence of neutrophils and macrophages. Migration of the neutrophils and macrophages toward the wound area were observed at 4-hour post amputation with inflammatory response. **c** The effect of ginsenoside Rg1 on inhibiting migration of neutrophils and macrophages, in comparison to the beclomethasone as a positive control. **d–e** The effect of Rg1 on expression of genes that relate to inflammation and innate immune system. Each collected sample includes 15 zebrafish larvae for the qPCR tests. For all experiments, three independent replicates were performed. The error bars indicate standard deviations of the median in each group.

At the transcriptional level, the gene expression of inflammatory cytokines (TNF-α, IL-1β, and IL-8), chemokines (CXCL18b, CXCL11aa, and CCL2), the inhibitor of nuclear factor-κ B (IκB), and MMP-9 was measured 4 hours after tail amputation using quantitative reverse transcription PCR (RT-qPCR) analysis. These results indicated that amputation induced the expression of all examined inflammatory genes, except for CCL2, which was significantly downregulated in the amputated group (▶ **Fig. 1 d, e**). Treatment with beclomethasone significantly downregulated IL-1β, IL-8, CXCL18b, and MMP9, but upregulated IκB. No effect was observed on TNF-α, CXCL11aa, and CCL2 in the amputated larva. Both Rg1 and beclomethasone downregulated the gene induction of IL-1β, CXCL18b, and MMP9, suggesting common targets for the anti-inflammatory effects of Rg1 and beclomethasone (▶ **Fig. 1 c, d**). However, they increased the expression of IκB. Intriguingly, only Rg1 inhibited the expression of the chemokine-encoding gene for CXCL11aa, indicating potential differences between the activities of beclomethasone and Rg1 in the regulation of chemokine-encoding gene expression.

Metabolomics provides a systems-like approach for the evaluation of the wound-injury of zebrafish larva and of the potential differences in immune-metabolism changes induced by Beclo and Rg1. To identify metabolites of interest, a non-targeted metabolomics approach was applied to the data obtained from the total ion chromatogram (TIC) of all samples resulting from their GC-MS analysis (Supplementary **Fig. 1S**). This technique is characterized by its large peak capacity and reproducibility of retention times, a clear indication of its reliability for metabolomics analysis. A total number of 110 metabolites were identified, including various primary metabolites such as amino acids, organic acids, carbohydrates, fatty acids, purine, pyrimidine and phosphate derivatives. The visual inspection of chromatograms showed differences in the profiles of the NA, AMP, and drug-treated groups (Beclo and Rg1). A principal component analysis (PCA) was conducted to monitor the effect of metabolic variables on the group classifications. To enhance the group separation and to further analyze which variables responded to these separations, PLS-DA, a supervised method, was performed on the data matrixes. A clear separation among the four groups was obtained as shown by the score plot in ▶ **Fig. 2 a**, indicating distinct group classifications for all groups and treatments. The first two principal components (PC1 and PC2) represented 20% of the total variance of the metabolome (model statistics: $R^2X = 0.396$, $R^2Y = 0.854$, and $Q^2 = 0.571$), indicating a good performance of the model without overfitting for the clear separation according to the cross-validation test. The *p*-value of the CV-ANOVA test indicated the significance of

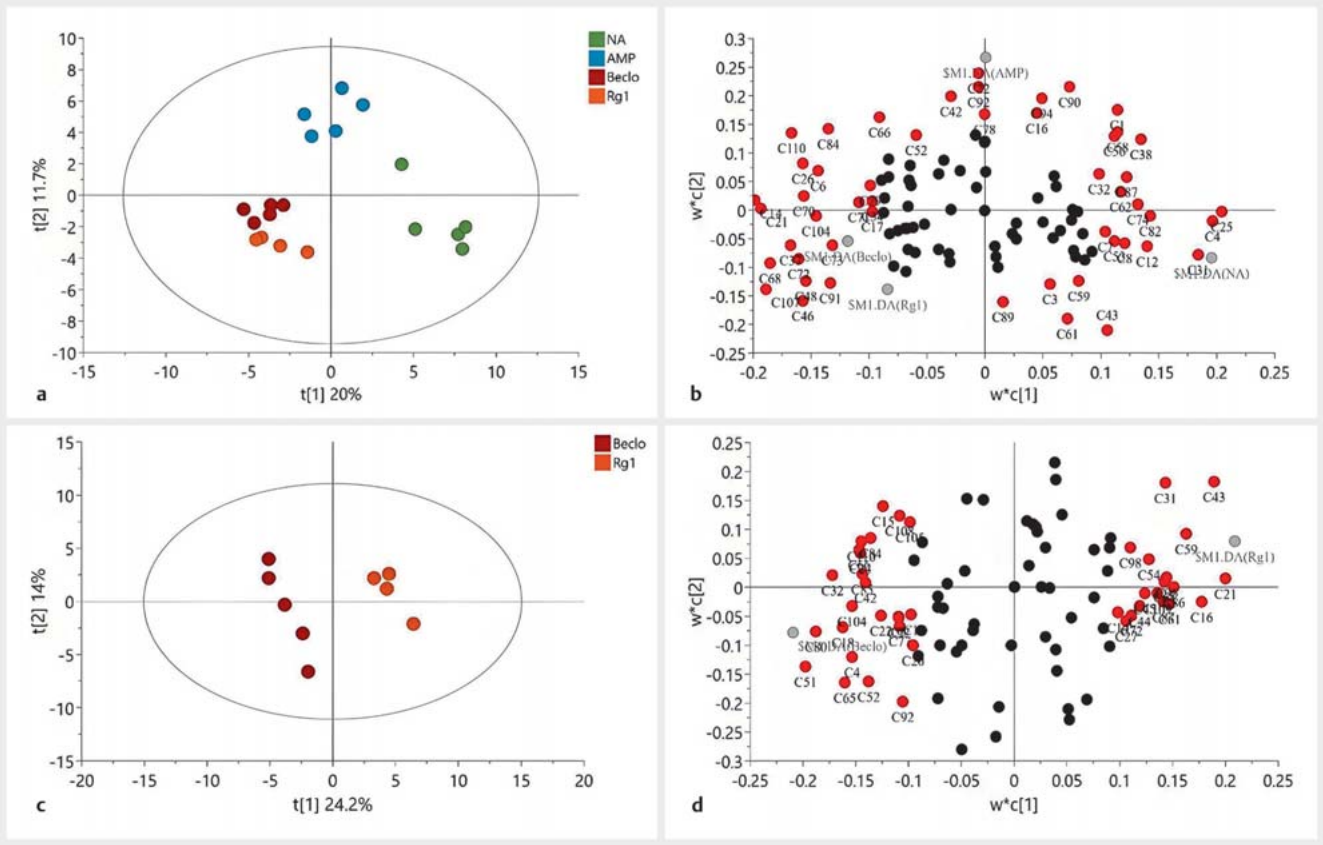

▶ **Fig. 2** PLS-DA score plots for the classification among different groups. **a** PLS-DA score plot based on 110 primary metabolites measured by GC–MS; **b** Primary metabolites that response to the relative group classifications (VIP score > 1 in red); **c** PLS-DA score plot based on 110 primary metabolite measured by GC–MS; **d** Loading plot of C shows primary metabolites that response to the group classification (VIP score > 1 in red); NA: no amputation + vehicle, AMP: amputation + vehicle, Beclo: amputation + beclomethasone, Rg1: amputation + Rg1.

the PLS-DA model ($p < 0.005$). A loading plot (▶ **Fig. 2b**) displayed the important variables that were contributed to the sample scatters (marked in red).

Another PLS-DA model was conducted to further identify the potential metabolic differences that were responsible for the separation between the Rg1 treatment and the beclomethasone treatment, and the loading plot of PLS-DA was applied to the score plot of PLS-DA (▶ **Fig. 2c, d**). The score plots (model statistics: $R^2X = 0.382$, $R^2Y = 0.988$, and $Q^2 = 0.757$) indicated a clear separation between the two drug-treated groups, without too much overfitting according to the cross-validation with 100 permutation tests and intercepts (model statistics: $R^2X = 0.396$, $R^2Y = 0.854$, and $Q^2 = 0.571$), respectively (see Supplementary **Fig. 3S**). These results, together with the previous inflammatory study, indicate that under inflammatory condition, the immune response is accompanied with a large scale of metabolic disorders, which can be restored by the Rg1 treatment revealed by metabolomics analysis.

Metabolomics offers a systems-level approach for evaluating wound injury in zebrafish larvae and discerning potential differences in immune-metabolism changes induced by Beclo and Rg1. To identify metabolites of interest, a non-targeted metabolomics approach was applied to the data obtained from the total ion chromatogram (TIC) of all samples resulting from their GC-MS analysis (Supplementary **Fig. 1S**). Generated chromatograms, characterized by their substantial peak capacity and reproducibility of retention times, demonstrate reliability for metabolomics analysis. A total of 110 metabolites were identified, encompassing various primary metabolites such as amino acids, organic acids, carbohydrates, fatty acids, purines, pyrimidines, and phosphate derivatives.

Visual inspection of chromatograms revealed differences in the profiles of the NA, AMP, and drug-treated groups (Beclo and Rg1). Principal component analysis (PCA) was conducted to monitor the effect of metabolic variables on group classifications. To enhance group separation and analyze variables responding to these separations, partial least squares discriminant analysis (PLS-DA), a supervised method, was performed on the data matrices. The score plot in ▶ **Fig. 2a** demonstrated a clear separation among the four groups, indicating distinct group classifications for all groups and treatments. The loading plot (▶ **Fig. 2b**) displayed important variables contributing to the sample scatters, marked in red.

To investigate metabolites responsible for the groups, an unsupervised method, the PLS-DA model, was conducted to further identify potential metabolic differences responsible for the separation between Rg1 treatment and beclomethasone treatment.

The loading plot of PLS-DA was applied to the score plot of PLS-DA (▶ **Fig. 2c,d**). The score plots (model statistics: R2X = 0.382, R2Y = 0.988, and Q2 = 0.757) indicated a clear separation between the two drug-treated groups, with minimal overfitting according to cross-validation with 100 permutation tests and intercepts (model statistics: R2X = 0.396, R2Y = 0.854, and Q2 = 0.571), respectively (see Supplementary **Fig. 3S**). These findings, combined with the previous inflammatory study, suggest that under inflammatory conditions, the immune response is accompanied by a large-scale metabolic disorder, which can be restored by Rg1 treatment, as revealed by metabolomics analysis.

To explore the key metabolites contributing to group classification, 25 metabolites were further filtered and defined as significant biomarkers using the threshold variable importance in project plot (VIP) > 1 from the PLS-DA model. These were further confirmed with a Student's *t*-test between each of the two groups (▶ **Table 1**). The filtered metabolite profiles with their regulation trends are presented in ▶ **Table 1**. Levels of 16 metabolites were significantly modified in the AMP group versus the NA group, including seven amino acids (salicyluric acid, glycine, isoleucine, proline, phenylalanine, glutamine, and tyrosine), a sugar (mannose), seven organic acids (malic acid, lactic acid, butanoic acid, hexadecanoic acid, octadecanoic acid, aminomalonic acid, and uric acid), and an inorganic acid (phosphoric acid). Most detected amino acids (six out of seven) were downregulated, while the remaining 10 metabolites were upregulated in the AMP group. Compared with AMP, beclomethasone significantly regulated 12 metabolites such as proline, galactose, *myo*-inositol, seven organic acids (malic acid, fumaric acid, lactic acid, hexadecane, aminomalonic acid, tricarballylic acid, and uric acid), phosphoric acid, and adenosine. Among these metabolites, six metabolites (galactose, myo-inositol, fumaric acid, hexadecane, tricarballylic acid, and adenosine) were significantly regulated by beclomethasone but did not significantly differ in the inflammatory amputation. The beclomethasone treatment downregulated only three organic acids (malic acid, lactic acid, and phosphoric acid), which were significantly elevated after the tail amputation with inflammatory response (▶ **Table 1**). Additionally, beclomethasone even downregulated proline levels that were decreased by amputation and upregulated the levels of aminomalonic acid and uric acid, which were elevated by amputation.

In contrast, more metabolites (n = 22) were regulated by the Rg1 treatment, exceeding the number regulated by beclomethasone. Specifically, five amino acids (salicyluric acid, glycine, phenylalanine, glutamine, and tyrosine), five sugars (mannose, galactose, galactopyranose, glucose, and myo-inositol), nine organic acids (malic acid, fumaric acid, lactic acid, hexadecane, hexadecanoic acid, octadecanoic acid, aminomalonic acid, tricarballylic acid, and uric acid), two purine-derived metabolites (isoxanthopterin and adenosine), and phosphoric acid were regulated by Rg1. Among these significant metabolites, three amino acids (phenylalanine, glutamine, and tyrosine), mannose, four organic acids (malic acid, lactic acid, hexadecanoic acid, and octadecanoic acid), and phosphoric acid that were dysregulated by inflammatory amputation were significantly restored by Rg1. This may suggest that Rg1 regulates differently from beclomethasone at the metabolic level and may have more beneficial effects on wound-injured zebrafish. To further gain a better understanding of how metabolic pathways are influenced by Rg1 regulation under inflammatory conditions, the KEGG website was utilized to construct pathways crucial in the inflammatory response and metabolic disorders based on significant changes observed in biomarkers (see ▶ **Table 1** and **Fig. 3**). These biomarkers were primarily associated with 14 metabolic pathways: amino sugar and nucleotide sugar; fructose and mannose; starch and sucrose; glycine, serine, and threonine; glutamine and glutamate; arginine and proline; phenylalanine, tyrosine, and tryptophan biosynthesis; tyrosine; pyrimidine; the citrate cycle (TCA cycle); pyruvate; fatty acid; inositol phosphate; purine metabolism (▶ **Fig. 4**). Among these pathways, both Rg1 and beclomethasone exhibited similar regulation in galactose metabolism, inositol phosphate metabolism, TCA cycle, pyruvate metabolism, fatty acid metabolism, and purine metabolism. However, Rg1 regulated additional pathways such as phenylalanine, tyrosine, and tryptophan metabolism, glycine, serine, and threonine metabolism, glutamine and glutamate metabolism, and sugar metabolism (e.g., glucose metabolism; fructose and mannose metabolism; amino sugar and nucleotide sugar metabolism).

Discussion

Inflammation, typically considered detrimental, plays a crucial role in tissue repair following injury, an essential aspect of the healing process. Neutrophils and macrophages, integral to this process, contribute to both immune and non-immune functions. In our investigation, Rg1 exhibited potential anti-inflammatory activity by restraining immune cell migration and suppressing the gene expression of pro-inflammatory cytokines (il1b, cxclc1c, and mmp9) in the amputated tail of zebrafish larvae. Notably, we observed potential differences in their regulatory pathways, both upstream and downstream. Specifically, Rg1 impacted both neutrophils and macrophages, while beclomethasone predominantly affected neutrophils. Additionally, Rg1 demonstrated differential effects on the gene expression of il8, cxcl11aa, and ccl2 compared to beclomethasone. These findings suggest potential divergences in the regulatory mechanisms against inflammatory response between Rg1 and beclomethasone.

To delve deeper into the intrinsic regulatory distinctions between the actions of these two drugs, we employed GC-MS combined with pattern recognition technology to analyze metabolic profiles. Substantial differences were identified in the species and concentration levels of significant metabolites, indicative of distinct involvement in well-discriminated metabolic pathways. Further analysis revealed additional pathway variances, particularly those related to energy imbalances, encompassing the regulation of glycolysis, amino acids, fatty acids, and lipids and another intermediate metabolism.

Galactose contributes to ATP production through glycolysis and participates in the recycling of NADH, promoting rapid ATP generation during cellular activation. However, elevated galactose levels are associated with pathological processes, including the production of reactive oxygen species (ROS) and the accumulation of advanced glycation end products (AGE), contributing to diseases such as diabetes, atherosclerosis, nephropathy, infection, and Alzheimer's [22]. Some studies also suggest a correlation be-

▶ **Table 1** Significant changed metabolites response to different drug treatments in the amputated zebrafish.

Group	Metabolites	RT	Regulation (AMP vs. NA)	Regulation (Beclo vs. AMP)	Regulation (Rg1 vs. AMP)	Pathway
Amino acid	Salicyluric acid (C4)	7.496	↓ *	–	↓ **	Phenylalanine metabolism
	Glycine (C14)	10.969	↑ **	–	↑ *	Glycine, serine, and threonine metabolism
	Isoleucine (C12)	10.729	↓ *	–	–	Valine, leucine, and isoleucine biosynthesis
	Proline (C25)	14.86	↓ **	↓ *	–	Arginine and proline metabolism
	Phenylalanine (C31)	16.651	↓ **	–	↑ *	Phenylalanine, tyrosine, and tryptophan biosynthesis
	Glutamine (C43)	18.991	↓ **	–	↑ **	Glutamine and glutamate metabolism
	Tyrosine (C61)	21.429	↓ *	–	↑ *	Phenylalanine, tyrosine, and tryptophan biosynthesis
Saccharide	Mannose (C92)	27.156	↑ *	–	↓ *	Fructose and mannose metabolism
	Galactose (C48)	20.044	–	↑ *	↑ *	Galactose metabolism
	Galactopyranose (C58)	20.931	–	–	↓ *	Amino sugar and nucleotide sugar metabolism
	Glucose (C102)	29.972	–	–	↑ *	Glucose metabolism
	Myo-Inositol (C94)	27.483	–	↓ *	↓ *	Inositol phosphate metabolism
Organic acids	Malic acid (C22)	14.311	↑ **	↓ *	↓ **	TCA-Cycle
	Fumaric acid (C16)	11.816	–	↓ **	↓ *	TCA-Cycle
	Lactic acid (C1)	5.991	↑ *	↓ *	↓ **	Pyruvate metabolism
	Butanoic acid (C26)	15.043	↑ *	–	–	Butanoate metabolism
	Hexadecane (C91)	27.099	–	↑ **	↑ *	Fatty acid metabolism
	Hexadecanoic acid (C66)	22.968	↑ *	–	↓ **	Fatty acid metabolism
	Octadecanoic acid (C84)	25.509	↑ **	–	↓ *	Fatty acid metabolism
	Aminomalonic acid (C21)	13.967	↑ *	↑ *	↑ **	TCA-Cycle
	Tricarballylic acid (C46)	19.684	–	↑ **	↑ **	TCA-Cycle
	Uric acid (C68)	23.62	↑ **	↑ **	↑ *	Purine metabolism
Purin and pyrimidine	Isoxanthopterin (C72)	24.078	–	–	↑ *	Purine metabolism
	Adenosine (C107)	34.498	–	↑ **	↑ **	Purine metabolism
Phosphate derivatives	Phosphoric acid (C6)	18.808	↑ *	↓ *	↓ **	TCA-Cycle

The sequence of the metabolites indicates their importance for the contribution to the group separations; ↑: increase; ↓: decrease; –: no significant change; *: $p < 0.05$, **: $p < 0.01$, Structural unidentified metabolites in GC-MS untargeted measurement

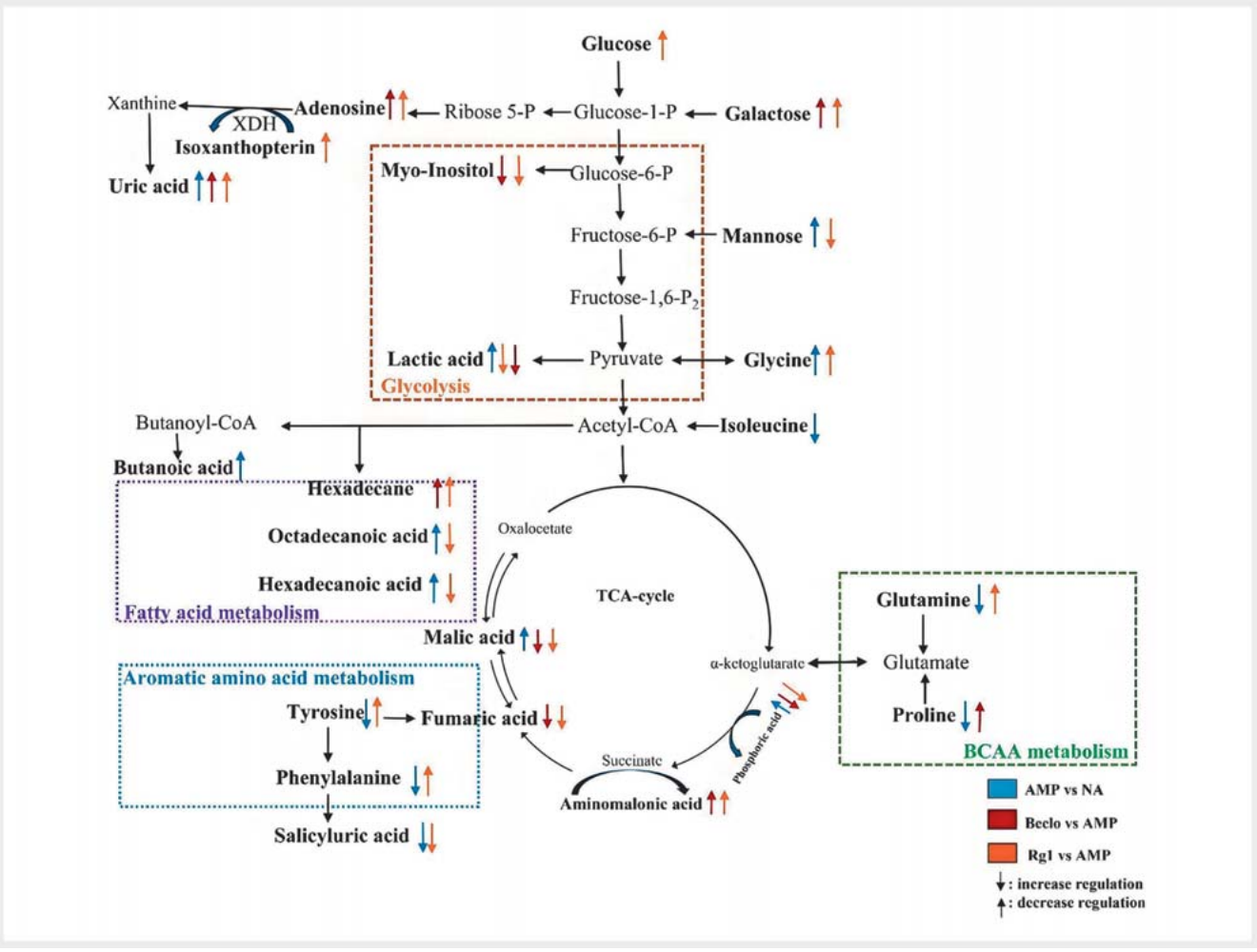

▶ **Fig. 3** Concentrations of significantly different metabolites detected by GC-MS, compared among different groups. The peak areas were normalized to the internal standard methyl palmitate in each sample. Analysis of variance (ANOVA) and Fisher's least-significant difference (LSD) *post hoc* test were performed for the comparison between groups. * $p < 0.05$.

tween galactose and proinflammatory mediators (IL-6 and TNF-α), leading to lipid peroxidation [23]. Additionally, under hypoxic conditions, increased lactic acid production, linked to glutamine-carbon overflow, is considered a potential biomarker of ischemia and hypoxia, which are found to be elevated in patients with acute ischemic stroke (AIS) under inflammatory conditions [24].

This study clearly revealed that Rg1 and beclomethasone significantly reduced elevated lactic acid levels under inflammatory conditions, potentially indicating their capacity to regulate carbohydrate metabolism and prevent excessive ammonia accumulation. Moreover, similar to beclomethasone, Rg1 demonstrated regulatory effects not only on sugar metabolism (e.g., galactose) but also on carbohydrates (up-regulating upstream glucose and galactose while down-regulating downstream mannose), modulating energy intake and adjusting activity to reduce ATP requirements.

Adenosine, crucial for wound healing and angiogenesis, stimulates the immune and inflammatory system by binding to cell-surface adenosine receptors (A1, A2A, A2B, and A3) [25]. Our results indicate that Rg1 significantly upregulates adenosine production but it downregulates downstream uric acid, along with isoxanthopterin, a vital cofactor in cell metabolism. This aligns with our previous findings suggesting that Rg1 facilitates wound healing after tail-fin amputation.

Given the regulation of Rg1 and beclomethasone on sugar/carbohydrate metabolism, it is logical to examine their influence on downstream TCA and amino acid metabolism pathways. Our results demonstrate that Rg1's down-regulation of malic and fumaric acids leads to the accumulation of their intermediate metabolite, tricarboxylic acid (TCA), favoring the regulation of energy metabolism in mitochondria. These metabolites can subsequently participate in amino acid metabolism after the TCA cycle.

Moreover, there is a growing body of evidence linking amino acids to the inflammatory response to injury, demonstrating not only an increase in the expression of anti-inflammatory cytokines and tight junction proteins but also a reduction in oxidative stress [26]. This aligns with our study's findings, revealing a decrease in the levels of specific amino acids, including salicyluric acid, isoleucine, proline, phenylalanine, glutamine, and tyrosine, in the am-

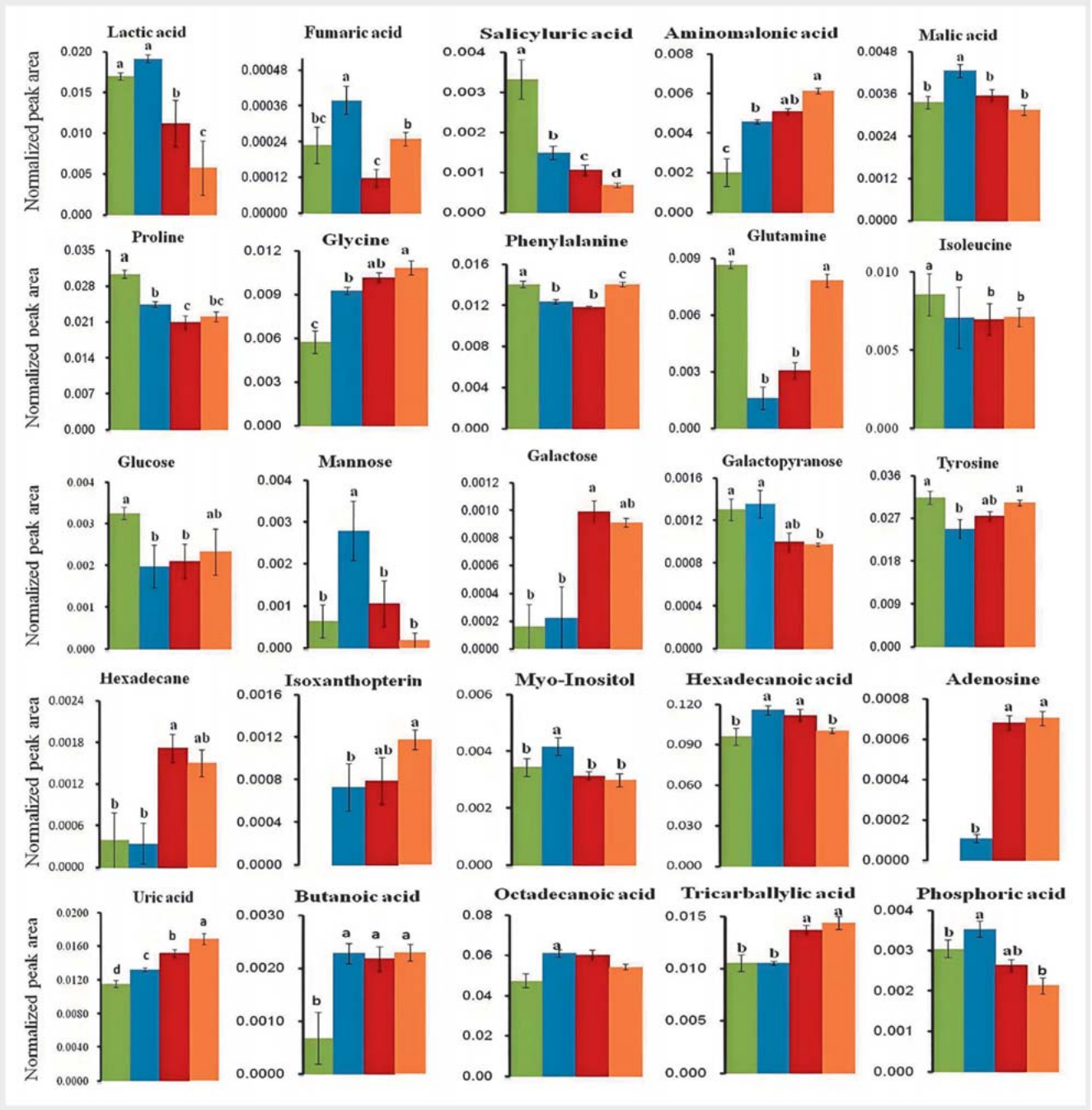

▶ **Fig. 4** Metabolic changes under inflammatory situation and the changed primary pathways under the drug treatment. The error bars indicate standard deviations of the median in each group. Green color indicates the control group. Amputated model group were displayed in blue color. The positive control group was treated with beclomethasone and was displayed in red color. The orange color indicates the Rg1 treatment. Each collected sample includes 15 zebrafish larvae, and each test group includes 3 replicates for detection, indicating a total 45 zebrafish information for metabolic analysis.

putated (AMP) samples. This observation underscores the involvement of amino acids in the regulation of energy metabolism, leading to significant flux changes in the tricarboxylic acid cycle (TCA), consistent with previous reports on various inflammatory diseases [24, 27].

Among the mentioned amino acids, isoleucine and glutamine are particularly noteworthy. These amino acids are major metabolic products derived from branched-chain amino acids (BCAAs), including leucine and valine. BCAAs serve numerous physiological and metabolic functions, such as promoting protein synthesis and renewal, mediating signal transduction pathways, and influencing

glucose metabolism. They also play crucial roles in the immune system and brain functions. Clinical supplementation with BCAAs has been shown to be beneficial for patients with liver disease, renal failure, sepsis, and surgical injury [28]. Additionally, BCAAs serve as the main nitrogen source for the synthesis of glutamine and alanine in muscle tissue [29].

Glutamine, being the most abundant amino acid, regulates acid-base homeostasis and gluconeogenesis. It also acts as a "nitrogen shuttle" between organs due to its buffering capacity. Functioning as a buffer, glutamine can accept excess ammonia and release it as needed to form other amino acids, amino sugars, nucleotides, and urea. This property protects the organism from elevated ammonia concentrations and contributes to rapid cell division and immune system regulation and serves as a precursor for nucleotide synthesis. The multifaceted functions of glutamine explain its reduction in plasma and muscles during conditions such as sepsis, cancer, cachexia, burn injury, and trauma [29]. This reduction in energetic glutamine and proline observed under inflammatory conditions in our study is consistent with these findings.

In this study, we observed that Rg1 upregulates glutamine and proline, influencing the glutamine and glutamate metabolism within the TCA cycle pathway. This suggests an immunomodulatory effect of ginseng by accelerating the accumulation of branched-chain amino acids (BCAAs), in addition to its known anti-inflammatory properties. Previous studies have reported immunomodulatory effects of ginseng extracts and ginsenosides on innate immunity [30]. Moreover, proline and glycine are recognized as primary precursors for collagen synthesis, playing essential roles in cell-mediated wound healing and injury recovery [31]. Glycine, in particular, affects immune responses in various immune cells, exhibiting anti-inflammatory and cytoprotective effects [32] and enhancing liver regeneration in patients following hepatectomy [33]. Our results indicate that Rg1 upregulates glycine levels, while beclomethasone further downregulates proline levels. This may explain our earlier observation that Rg1, acting as an anti-inflammatory drug candidate, does not exhibit glucocorticoid-like tissue regeneration.

The increase in both glutamate and glycine metabolite levels in mice treated with Asian ginseng, as observed in other studies [34], aligns with our findings. Importantly, our results highlight that inflammation induces changes in the metabolism of aromatic amino acids, particularly tryptophan and phenylalanine. Phenylalanine, being an essential amino acid and a precursor of crucial metabolites such as tyrosine, dopamine, norepinephrine, and epinephrine, undergoes metabolism via tyrosine to yield acetoacetic acid and fumaric acid [35]. Our study revealed downregulation of phenylalanine and tyrosine in inflamed zebrafish and their upregulation with Rg1 treatment, suggesting accelerated TCA cycle activity involving fumaric acid and malic acid metabolism. This observation aligns with other studies confirming that the phenylalanine/tyrosine pair may serve as important biomarkers of inflammation and acute ischemic stroke (AIS) [36].

In fatty acid metabolism, acetyl-coenzyme A (Acetyl-CoA), a byproduct of sugar metabolism, along with its carboxylate derivative malonic acid monoacyl-CoA, can be transported outside the mitochondria via the tricarboxylic acid (TCA) cycle. Subsequently, long-chain fatty acids, encompassing both saturated and unsaturated varieties, undergo further synthesis. Notably, long-chain fatty acids, particularly unsaturated fatty acids, have been implicated in inflammation and the congenital immune response in human macrophages [37]. Unsaturated fatty acids can undergo oxidation, such as beta-oxidation, participating in diverse metabolic processes, including hormone regulation and the production of inflammatory cytokines, which contribute to the development of various inflammatory diseases [38–39]. Interestingly, beyond the observed amine-derived and sugar metabolic changes induced by Rg1, we have also identified its impact on the regulation of fatty acid metabolism disorders. Elevated levels of two saturated long-chain fatty acids, hexadecanoic acid (palmitic acid) and octadecanoic acid, were detected under inflammatory conditions, a phenomenon significantly attenuated by Rg1 but not by beclomethasone. This suggests the potential of Rg1 to mitigate inflammatory diseases, presenting a novel avenue for future exploration.

In this study, the zebrafish model has offered insights into Rg1′s metabolic effects, indicating its potential to modulate body metabolism. Although zebrafish embryos are valuable for studying inflammation and the metabolic effects of Rg1, their direct application to human contexts still face challenges due to physiological differences. Our findings in this study encourage the use of the zebrafish model for exploring Rg1′s metabolic effects and provide a nuanced perspective on the future translatability of these findings to mammalian and human applications. Based on the research outcomes of this article, our future work will confidently carry out studies on the regulatory effects of Rg1 on more metabolic diseases. Furthermore, we plan to continue verifying the relevant pharmacological effects through mammalian experiments and clinical trials and to explore the possibility of their transformation into practical applications.

In summary, this study contributes additional scientific evidence supporting the potential anti-inflammatory effect of Rg1, which shares similarities with the glucocorticoid beclomethasone but exhibits significant differences in their metabolic mechanisms concerning injury-wounded zebrafish. Beclomethasone, a widely recognized anti-inflammatory glucocorticoid, primarily influences upstream energy metabolism, specifically monosaccharides and intermediates, thereby regulating the tricarboxylic acid (TCA) cycle. In contrast, Rg1 predominantly targets fatty acids and downstream amino acids in the TCA cycle, playing diverse roles not only as cell signaling molecules but also as regulators of inflammatory and immune responses. The extensive metabolic pathways affected by Rg1 administration encompass phenylalanine, tyrosine, and tryptophan biosynthesis, glycine, serine, and threonine metabolism, glutamine and glutamate metabolism, pyruvate metabolism, inositol phosphate metabolism, and purine metabolism. The broad regulation of downstream TCA amino acids and fatty acids by Rg1 provides additional evidence supporting Rg1 as a promising drug candidate against inflammatory responses and as a supplement for enhancing immunomodulation concurrently.

Materials and Methods

Chemicals and reagents

All chemicals employed in this study were of analytical grade. Internal standards and reagents for GC-MS analysis, namely N,O-Bis (trimethylsilyl) trifluoroacetamide (BSTFA) plus 1% trimethylchlorosilane (TMCS) were purchased from Pierce Chemical Co., and beclomethasone was procured from Sigma-Aldrich Co. The Rg1 reference compound (purity > 98%) was sourced from Solarbio Science & Technology Co., Ltd.

Zebrafish treatments

Zebrafish (*Danio rerio*) of the transgenic line *Tg* (mpx:GFPi114/mpeg1:mcherry-FumsF001) were sourced and maintained at the Institute of Biology Leiden (IBL) in Leiden University. The animal study received approval from the Institutional Animal Care and Use Committee of Leiden University, the Netherlands, (license number 10612) under protocol 14198 and adhered to the standard guidelines from the Zebrafish Model Organism Database (https://zfin.org, accessed on 30 January 2023).

Three-day-old zebrafish larvae were cultured in egg water (containing 60 g/mL Instant Ocean Sea salts and 0.0025% methylene blue) and treated with 120 µM Rg1 or 25 µM beclomethasone (Beclo, used as a positive control) two hours before inducing acute inflammation through tail-fin amputation (▶ **Fig. 1 a**) [40]. The use of the Rg1 dosage was informed by our previous study, which found that a significant effect begins when the dose exceeds 100 µM, equivalent to the effect of beclomethasone at doses higher than 120 µM. Consequently, a concentration of 120 µM was used for the metabolomics study presented in this study. The experiments were set up in a 24-well plate with 15 larvae in each well, divided into four groups: (a) control group without amputation to the larvae (NA group), (b) vehicle treatment after amputation (Amp + vehicle), (c) beclomethasone treatment after amputation (Amp + Beclo), and (d) Rg1 treatment after amputation (Amp+Rg1). The experiment was performed in quintuplicate.

For tail-fin amputation, embryos were anesthetized with tricaine (buffered 0.02% aminobenzoic acid ethyl ester in egg water) and placed on Petri dishes coated with 2% agarose. The tail fin of each larva was amputated (▶ **Fig. 1 a**) using a 1 mm sapphire blade under a Leica MZ16FA fluorescence stereomicroscope. Neutrophils and macrophages in the wounded area were tracked by GFP and mCherry fluorescence, respectively (▶ **Fig. 1 b**), and quantified. Four hours after amputation, the zebrafish larvae were quickly rinsed twice with water, transferred to 2 mL centrifuge tubes, and snap-frozen in liquid nitrogen. The larval samples were stored at − 20 °C until further processing.

RT-qPCR

Gene expression at the transcriptional level was assessed through the RT-qPCR (reverse transcription–quantitative PCR) method. RNA isolation was carried out using TRIzol reagent (Invitrogen) following the manufacturer's instructions. The initial cDNA strand was synthesized using the iScript cDNA synthesis kit and subsequently subjected to qPCR analysis, employing the amplification conditions as previously described [21]. Each collected sample includes 15 zebrafish larvae for the qPCR tests. For all experiments, three independent replicates were performed. The error bars indicate standard deviations of the median in each group.

Metabolites extraction for GC-MS analysis

Zebrafish larvae were treated following a previously documented procedure [41]. The frozen zebrafish larval samples were combined with 1 mL of methanol and sonicated at room temperature for 30 minutes, after which centrifugation at 13000 rpm/min (18894.2 ×g) for 10 minutes was conducted. The supernatant was collected and subjected to drying in a Speed-vac (ThermoScientific). The resultant dried extract was reconstituted in 100 µL of anhydrous pyridine and derivatized using 100 µL of *N, O*-Bis-(trimethylsilyl) trifluoroacetamide (BSTFA) and 1% trimethylchlorosilane (TMCS) at 80 °C for 50 minutes. Following derivatization, the extract was combined with 50 µL of an internal standard solution (1 mg/mL methylpalmitate dissolved in pyridine) and centrifuged at 13000 rpm/min (18894.2 ×g) for 5 minutes at room temperature prior to GC/MS analysis.

GC–MS analysis

The derivatized zebrafish larval sample underwent analysis using a 7890A gas chromatograph mass spectrometer equipped with a 7693 automatic sampler and a 5975C single-quadrupole detector (Agilent). The sample was injected onto a DB-5 GC column (30 m × 0.25 mm, 0.25 µm film, J&W Science) and eluted with Helium (99.9% purity) as a carrier gas at a flow rate of 1 mL/min. The initial temperature was set at 40 °C, and it was increased to 150 °C at a rate of 5 °C/min, followed by an increase to 260 °C at 7 °C/min, with a 3-minute hold. The injector was maintained at 250 °C, and 1 µL of the sample was injected in the split mode (10:1). The interface temperature was 280 °C, and the ion source and quadrupole temperatures of the mass detector were set at 230 °C and 150 °C, respectively. Ionization energy in EI mode was 70 eV. Peaks were identified through a comparison of ion spectra with the NIST library version 2008 (https://www.nist.gov/srd) or by comparing retention times and spectra with those of standard compounds. Methyl palmitate served as the internal standard with a final concentration of 100 ng/µL.

Data processing and statistical analysis

Inflammatory marker data are presented as the mean ± standard error of the mean (SEM). Group comparisons were conducted using analysis of variance (ANOVA) and Fisher's least-significant difference (LSD) *post hoc* test. An independent *t*-test was employed for comparisons between Amp vs. NA groups and treated vs. untreated samples. A P value < 0.05 was considered statistically significant.

All total ion chromatograms (TIC) were automatically integrated, and peak identification was performed using Mass Hunter Qualitative Analysis software version B.07.00 (Agilent). Files in 'CDF' format obtained from GCMS, containing sample information such as retention time and peak intensity, were exported to Microsoft Excel for further preprocessing. The internal standard was used for data quality control to ensure reproducibility. Peaks corresponding to the internal standard and any identified in blank samples were removed from the dataset. Normalization of the dataset

was carried out by the total intensity of peaks in each sample for multivariate data analysis (MVDA) using SIMCA P software (Version 15.1, Umetrics, Umeå Sweden). Data scaling was performed using the Pareto method. Partial least squares discriminant analysis (PLS-DA), a supervised method, was utilized for maximum classification, separation of independent samples, and feature selection based on R^2X, R^2Y, and Q^2Y. A permutation test (100 substitutions in all models) was employed to assess the validity of the PLS-DA model for overfitting. Metabolite pattern analysis followed the approach described by Xia et al. 2015 [42]. The Variable Importance in the Projection (VIP) score was calculated in the PLS-DA model. The identification of the most crucial metabolites was the primary discriminating feature distinguishing between the Amp and NA groups, as well as between treated and Amp groups. Compounds with VIP values > 1.0 and p values < 0.05, as obtained from the PLS-DA scatter plot model, were considered potential biomarkers. Metabolic pathways associated with each potential biomarker were determined using the Kyoto Encyclopedia of Genes and Genomes (KEGG, http://genome.jp/kegg) [43].

Supporting information

Total ion chromatograms (TICs) for the metabolomics analysis by GC-MS, as well as the validation of the PLSDA model, are available as supporting information.

Contributors' Statement

Design of the study: M. He, M. Wang; Sample preparation: M. He; data collection and statistical analysis: S. Hsu, M. He; drafting the manuscript: S. Hsu, M. He, Y. H. Choi; critical revision of the manuscript: L. F. Salomé-Abarca, Y. H. Choi, M. Wang. All authors read and approved the final manuscript.

Funding Information

S.-J. Hsu received funding (MOST 107-2917-I-415-002) from the Graduate Students Study Abroad Program, Ministry of Science and Technology (Taiwan). Min He acknowledges the Jilin Provincial Development and Reform Commission (grant number 2023C028–1), the Scientific and Technological Developing Project of Jilin Province (grant number YDZJ202101ZYTS119), as well as the financial support of the Pilotscale Selection Project of Colleges and Universities in Changchun City (No. 24GXYSZZ10). Mei Wang would like to express her gratitude for the "Wang Mei Expert Workstation" of Yunnan Province (201905AF150001) and Yunnan Provincial Department of Science and Technology (project number: 202003AC100013).

Acknowledgements

We greatly appreciate Professor Annemarie Meijer from Leiden University for providing zebrafish embryos and experimental conditions and Professor Shu-Mei Lin from National Chiayi University for reviewing and modifying the manuscripts, and we appreciate Yangan Chen from Leiden University for her helpful suggestions and supporting data analysis. The researchers appreciate the help from Anna June van Duijn for her professional figure drawing for the schematic diagram of zebrafish in **1**.

Conflict of Interest

The authors declare that they have no conflict of interest.

References

[1] Furman D, Campisi J, Verdin E, Carrera-Bastos P, Targ S, Franceschi C, Ferrucci L, Gilroy DW, Fasano A, Miller GW, Miller AH, Mantovani A, Weyand CM, Barzilai N, Goronzy JJ, Rando TA, Effros RB, Lucia A, Kleinstreuer N, Slavich GM. Chronic inflammation in the etiology of disease across the life span. Nature medicine 2019; 25: 1822–1832. DOI: 10.1038/s41591-019-0675-0

[2] Baschant U, Tuckermann J. Journal of steroid biochemistry and molecular biology the role of the glucocorticoid receptor in inflammation and immunity. J Steroid Biochem Mol Biol 2010; 120: 69–75. DOI: 10.1016/j.jsbmb.2010.03.058

[3] Hu C, Lau AJ, Wang RQ, Chang T. Comparative analysis of ginsenosides in human glucocorticoid receptor binding, transactivation, and transrepression. Eur J Pharmacol 2017; 815: 501–511. DOI: 10.1016/j.ejphar.2017.10.019

[4] Vegiopoulos A, Herzig S. Glucocorticoids, metabolism and metabolic diseases. Mol Cell Endocrinol 2007; 275: 1–2

[5] Van Der Velden VHJ. Glucocorticoids: Mechanisms of action and anti-inflammatory potential in asthma. Mediators Inflamm 1998; 7: 229–237

[6] Lee YJ, Chung E, Lee KY, Lee YH, Huh B, Lee SK. Ginsenoside-Rg1, one of the major active molecules from Panax ginseng, is a functional ligand of glucocorticoid receptor. Mol Cell Endocrinol 1997; 133: 135–140. DOI: 10.1016/S0303-7207(97)00160-3

[7] Wishart D. Emerging applications of metabolomics in drug discovery and precision medicine. Nat Rev Drug Discov 2016; 15: 473–484

[8] Fuller H, Zhu Y, Nicholas J, Chatelaine HA, Drzymalla EM, Sarvestani AK, Julián-Serrano S, Tahir UA, Sinnott-Armstrong N, Raffield LM, Rahnavard A, Hua X, Shutta KH, Darst BF. Metabolomic epidemiology offers insights into disease aetiology. Nat Metab 2023; 5: 1656–1672

[9] Wheeler K, Gosmanov C, Sandoval MJ, Yang Z, McCall LI. Frontiers in mass spectrometry-based spatial metabolomics: Current applications and challenges in the context of biomedical research. Trends Analyt Chem 2024; online publication: 117713. DOI: 10.1016/j.trac.2024.117713

[10] Schauer N, Steinhauser D, Strelkov S, Schomburg D, Allison G, Moritz T, Lundgren K, Roessner-Tunali U, Forbes MG, Willmitzer L, Fernie AR, Kopka J. GC-MS libraries for the rapid identification of metabolites in complex biological samples. FEBS Lett 2005; 579: 1332–1337. DOI: 10.1016/j.febslet.2005.01.029

[11] Howe K, Clark MD, Torroja CF, Torrance J, Berthelot C, Muffato M, Collins JE, Humphray S, McLaren K, Matthews L, McLaren S, Sealy I, Caccamo M, Churcher C, Scott C, Barrett JC, Koch R, Rauch GJ, White S, Chow W, Kilian B, Quintais LT, Guerra-Assunção JA, Zhou Y, Gu Y, Yen J, Vogel JH, Eyre T, Redmond S, Banerjee R, Chi J, Fu B, Langley E, Maguire SF, Laird GK, Lloyd D, Kenyon E, Donaldson S, Sehra H, Almeida-King J, Loveland J, Trevanion S, Jones M, Quail M, Willey D, Hunt A, Burton J, Sims S, McLay K, Plumb B, Davis J, Clee C, Oliver K, Clark R, Riddle C, Elliot D, Threadgold G, Harden G, Ware D, Begum S, Mortimore B, Kerry G, Heath P, Phillimore B, Tracey A, Corby N, Dunn M, Johnson C, Wood J, Clark S, Pelan S, Griffiths G, Smith M, Glithero R, Howden P, Barker N, Lloyd C, Stevens C, Harley J, Holt K, Panagiotidis G, Lovell J, Beasley H, Henderson C, Gordon D, Auger K, Wright D, Collins J, Raisen C, Dyer L, Leung K, Robertson L, Ambridge K, Leongamornlert D, McGuire S, Gilderthorp R, Griffiths C, Manthravadi D, Nichol S, Barker G, Whitehead S, Kay M, Brown J, Murnane C, Gray E, Humphries M, Sycamore N, Barker D, Saunders D, Wallis J, Babbage A, Hammond S, Mashreghi-Mohammadi M Barr L, Martin S, Wray P, Ellington A, Matthews N, Ellwood M, Woodmansey R, Clark G, Cooper J, Tromans A, Grafham D, Skuce C, Pandian R, Andrews R, Harrison E, Kimberley A, Garnett J, Fosker N, Hall R, Garner P, Kelly D, Bird C, Palmer S, Gehring I, Berger A, Dooley CM, Ersan-Ürün Z, Eser C, Geiger H, Geisler M, Karotki L, Kirn A, Konantz J, Konantz M, Oberländer M, Rudolph-Geiger S, Teucke M, Lanz C, Raddatz G, Osoegawa K, Zhu B, Rapp A, Widaa S, Langford C, Yang F, Schuster SC, Carter NP, Harrow J, Ning Z, Herrero J, Searle SM, Enright A, Geisler R, Plasterk RH, Lee C, Westerfield

M, de Jong PJ, Zon LI, Postlethwait JH, Nüsslein-Volhard C, Hubbard TJ, Roest Crollius H, Rogers J, Stemple DL. The zebrafish reference genome sequence and its relationship to the human genome. Nature 2013; 496: 498–503. DOI: 10.1038/nature12111

[12] MacRae CA, Peterson RT. Zebrafish as a mainstream model for in vivo systems pharmacology and toxicology. Annu Rev Pharmacol Toxicol 2023; 63: 43–64. DOI: 10.1146/annurev-pharmtox-051421-105617

[13] Ali S, van Mil HGJ, Richardson MK. Large-scale assessment of the zebrafish embryo as a possible predictive model in toxicity testing. PLoS One 2011; 6: e21076. DOI: 10.1371/journal.pone.0021076

[14] Shimada Y, Kuroyanagi J, Zhang B, Ariyoshi M, Umemoto N, Nishimura Y, Tanaka T. Downregulation of Max dimerization protein 3 is involved in decreased visceral adipose tissue by inhibiting adipocyte differentiation in zebrafish and mice. Int J Obes 2014; 38: 1053–1060. DOI: 10.1038/ijo.2013.217

[15] Qin J, Ru S, Wang W, Hao L, Ru Y, Wang J, Zhang X. Long-term bisphenol S exposure aggravates non-alcoholic fatty liver by regulating lipid metabolism and inducing endoplasmic reticulum stress response with activation of unfolded protein response in male zebrafish. Environ Pollut 2020; 263: 114535. DOI: 10.1016/j.envpol.2020.114535. [Epub 2020 Apr 5] PMID: 32283406

[16] Vasyutina M, Alieva A, Reutova O, Bakaleiko V, Murashova L, Dyachuk V, Catapano AL, Baragetti A, Magni P. The zebrafish model system for dyslipidemia and atherosclerosis research: Focus on environmental/exposome factors and genetic mechanisms. Metabolism 2022; 129: 155138. DOI: 10.1016/j.metabol.2022.155138. Epub 2022 Jan 17. PMID: 35051509

[17] Cheng MC, Lee TH, Chu YT, Syu LL, Hsu SJ, Cheng CH, Wu J, Lee CK. Melanogenesis inhibitors from the rhizoma of ligusticum sinense in B16-f10 melanoma cells in vitro and zebrafish in vivo. Int J Mol Sci 2018; 19: 3994. DOI: 10.3390/ijms19123994

[18] Progatzky F, Sangha NJ, Yoshida N, McBrien M, Cheung J, Shia A, Scott J, Marchesi JR, Lamb JR, Bugeon L, Dallman MJ. Dietary cholesterol directly induces acute inflammasome-dependent intestinal inflammation. Nat Commun 2014; 5: 5864. DOI: 10.1038/ncomms6864

[19] Zang L, Maddison LA, Chen W. Zebrafish as a model for obesity and diabetes. Front Cell Dev Biol 2018; 6: 1–13. DOI: 10.3389/fcell.2018.00091

[20] Schaaf MJ, Champagne D, van Laanen IH, van Wijk DC, Meijer AH, Meijer OC, Spaink HP, Richardson MK. Discovery of a functional glucocorticoid receptor β-isoform in zebrafish. Endocrinology 2008; 149: 1591–1599. DOI: 10.1210/en.2007-1364

[21] He M, Halima M, Xie Y, Schaaf MJM, Meijer AH, Wang M. Ginsenoside Rg1 acts as a selective glucocorticoid receptor agonist with anti-inflammatory action without affecting tissue regeneration in zebrafish larvae. Cells 2020; 9: 1107. DOI: 10.3390/cells9051107

[22] Song X, Bao M, Li D, Li YM. Advanced glycation in D-galactose induced mouse aging model. Mech Ageing Dev 1999; 108: 239–251. DOI: 10.1016/S0047-6374(99)00022-6

[23] Hadzi-Petrushev N, Stojkovski V, Mitrov D, Mladenov M. D-galactose induced inflammation lipid peroxidation and platelet activation in rats. Cytokine 2014; 69: 150–153. DOI: 10.1016/j.cyto.2014.05.006

[24] Wang D, Kong J, Wu J, Wang X, Lai M. GC–MS-based metabolomics identifies an amino acid signature of acute ischemic stroke. Neurosci Lett 2017; 642: 7–13. DOI: 10.1016/j.neulet.2017.01.039

[25] Montesinos MC, Desai A, Chen JF, Yee H, Schwarzschild MA, Fink JS, Cronstein BN. Adenosine promotes wound healing and mediates angiogenesis in response to tissue injury via occupancy of A2A receptors. Am J Pathol 2002; 160: 2009–2018. DOI: 10.1016/S0002-9440(10)61151-0

[26] Monirujjaman M, Ferdouse A. Metabolic and physiological roles of branched-chain amino acids. Advances in Molecular Biology 2014; 2014: 364976–367982. DOI: 10.1155/2014/364976

[27] Ooi M, Nishiumi S, Yoshie T, Shiomi Y, Kohashi M, Fukunaga K, Nakamura S, Matsumoto T, Hatano N, Shinohara M, Irino Y, Takenawa T, Azuma T, Yoshida M. GC/MS-based profiling of amino acids and TCA cycle-related molecules in ulcerative colitis. Inflammation Research 2011; 60: 831–840. DOI: 10.1007/s00011-011-0340-7

[28] Ooi PH, Gilmour SM, Yap J, Mager DR. Effects of branched chain amino acid supplementation on patient care outcomes in adults and children with liver cirrhosis: A systematic review. Clin Nutr ESPEN 2018; 28: 41–51. DOI: 10.1016/j.clnesp.2018.07.012

[29] Holeček M. Relation between glutamine, branched-chain amino acids, and protein metabolism. Nutrition 2002; 18: 130–133. DOI: 10.1016/s0899-9007(01)00767-5

[30] Wang J, Hou Y, Jia Z, Xie X, Liu J, Kang Y, Wang X, Wang X, Jia W. Metabonomics approach to comparing the antistress effects of four panax ginseng components in rats. J Proteome Res 2018; 17: 813–821. DOI: 10.1021/acs.jproteome.7b00559

[31] Albaugh VL, Mukherjee K, Barbul A. Proline precursors and collagen synthesis: Biochemical challenges of nutrient supplementation and wound healing. Journal of Nutrition 2017; 147: 2011–2017. DOI: 10.3945/jn.117.256404

[32] Zhong Z, Wheeler MD, Li X, Froh M, Schemmer P, Yin M, Bunzendaul H, Bradford B, Lemasters JJ. L-Glycine: a novel antiinflammatory, immunomodulatory, and cytoprotective agent. Curr Opin Clin Nutr Metab Care 2003; 6: 229–240. DOI: 10.1097/00075197-200303000-00013

[33] Ito K, Ozasa H, Noda Y, Koike Y, Arii S, Horikawa S. Effect of non-essential amino acid glycine administration on the liver regeneration of partially hepatectomized rats with hepatic ischemia/reperfusion injury. Clin Nutr 2008; 27: 773–780. DOI: 10.1016/j.clnu.2008.06.012

[34] Yang L, Yu QT, Ge YZ, Zhang WS, Fan Y, Ma CW, Liu Q, Qi LW. Distinct urine metabolome after Asian ginseng and American ginseng intervention based on GC-MS metabolomics approach. Sci Rep 2016; 6: 39045. DOI: 10.1038/srep39045

[35] Wu G. Amino acids: Metabolism, functions, and nutrition. Amino Acids 2009; 37: 1–17. DOI: 10.1007/s00726-009-0269-0

[36] Wannemacher RW Jr, Klainer AS, Dinterman RE, Beisel WR. The significance and mechanism of an increased serum phenylalanine tyrosine ratio during infection. American Journal of Clinical Nutrition 1976; 29: 997–1006. DOI: 10.1093/ajcn/29.9.997

[37] Håversen L, Danielsson KN, Fogelstrand L, Wiklund O. Induction of proinflammatory cytokines by long-chain saturated fatty acids in human macrophages. Atherosclerosis 2009; 202: 382–393. DOI: 10.1016/j.atherosclerosis.2008.05.033

[38] Scott HA, Gibson PG, Garg ML, Wood LG. Airway inflammation is augmented by obesity and fatty acids in asthma. Eur Respir J 2011; 38: 594–602. DOI: 10.1183/09031936.00139810

[39] Wei X, Song H, Yin L, Rizzo MG, Sidhu R, Covey DF, Ory DS, Semenkovich CF. Fatty acid synthesis configures the plasma membrane for inflammation in diabetes. Nature 2016; 539: 294–298. DOI: 10.1038/nature20117

[40] Chatzopoulou A, Heijmans JP, Burgerhout E, Oskam N, Spaink HP, Meijer AH, Schaaf MJ. Glucocorticoid-induced attenuation of the inflammatory response in zebrafish. Endocrinology 2016; 157: 2772–2784. DOI: 10.1210/en.2015-2050

[41] Salomé-Abarca LF, van der Pas J, Kim HK, van Uffelen GA, Klinkhamer PGL, Choi YH. Metabolic discrimination of pine resins using multiple analytical platforms. Phytochemistry 2018; 155: 37–44. DOI: 10.1016/j.phytochem.2018.07.011

[42] Xia J, Sinelnikov IV, Han B, Wishart DS. MetaboAnalyst 3.0–making metabolomics more meaningful. Nucleic Acids Res 2015; 43: W251–W257. DOI: 10.1093/nar/gkv380

[43] Kanehisa M, Sato Y, Kawashima M, Furumichi M, Tanabe M. KEGG as a reference resource for gene and protein annotation. Nucleic Acids Res 2016; 44: D457–D462. DOI: 10.1093/nar/gkv1070